Design of Narrow-Band Photoreceivers by Means of the Photodiode Intrinsic Conductance

Andreas Leven, *Member, IEEE*, Volker Hurm, Ralf Reuter, and Josef Rosenzweig

***Abstract*—The photodiode intrinsic conductance is a versatile parameter for designing photoreceivers used in lightwave-microwave systems. A short review is given on how the transimpedance and equivalent input noise current of an optical receiver can be calculated. The design of monolithically integrated narrow-band photoreceivers for microwave-via-fiber applications at 10 GHz is demonstrated. The photoreceivers were fabricated using GaAs-based pseudomorphic high electron-mobility transistor monolithically integrated with metamorphic InGaAs photodiodes. For such a photoreceiver, a very low equivalent input noise current of 5.7 pA per square-root hertz and a high optoelectronic conversion gain of 64.1 dBV/W were measured in good agreement with simulations.**

***Index Terms*—Integrated optoelectronics, noise, optical receivers, photodetectors.**

I. Introduction

HYBRID LIGHTWAVE-MICROWAVE systems are expected to play an important role in future wireless communication systems and phased array antenna sensor systems [1]. One key component of such a system is the microwave photoreceiver front-end. Unlike photoreceivers used in digital baseband communication systems, photoreceivers used in microwave photonic systems are typically narrow-band with a bandwidth of 10% to 40% of the center frequency. This permits the use of reactive matching techniques to obtain optimum performance with respect to noise and conversion gain.

Several techniques are known for synthesizing matching networks that allow control of parameters like noise figure and gain of an amplifier during the design process. These techniques comprise simple methods like noise- and gain-circles in a Smith chart or much more advanced ones like the real frequency matching approach [2]. For the design of photoreceivers, only a few methods have been published, concentrating mainly on low-noise photoreceivers [3]–[6] and a few matching network topologies [7]. As the structure of a reactive matched photoreceiver is quite similar to that of a microwave/millimeter-wave amplifier, all methods for amplifier design should also be useful for the design of photoreceivers. For using these design techniques, the to-be-optimized figures like equivalent input noise current and conversion gain must be easily extractable from the figures used in microwave design, like scattering parameters and noise figure. The photodiode intrinsic conductance, introduced in [8], simplifies these calculations.

Manuscript received January 19, 2001; revised May 29, 2001. This work was supported by the German Ministry of Defense.

A. Leven was with the Fraunhofer-Institut für Angewandte Festkörperphysik, Freiburg, Germany. He is now with Lucent Technologies, Bell Laboratories, Murray Hill, NJ 07974 USA (e-mail: aleven@lucent.com).

V. Hurm and J. Rosenzweig are with the Fraunhofer-Institut für Angewandte Festkörperphysik, D-79108 Freiburg, Germany.

R. Reuter was with the Fraunhofer-Institut für Angewandte Festkörperphysik, Freiburg, Germany. He is now with the Semiconductor Products Sector, Motorola, D-13507 Berlin, Germany.

Publisher Item Identifier S 0018-9480(01)08712-9.

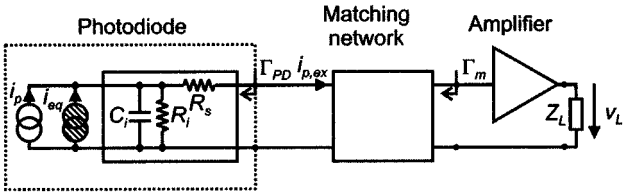

Fig. 1. Photoreceiver model comprising a photodiode, a matching network, and an amplifier.

In this paper, we show an application of this design approach by demonstrating the design of 10 GHz photoreceivers with very low equivalent input noise current and high conversion gain. These photoreceivers can be used in X-band phased array radar systems that are optically steered/feeded [9]. Receivers were fabricated using a GaAs-based technology that allows the monolithic integration of high electron mobility transistors (HEMTs) with long wavelength (1.55 μm) p-i-n-photodiodes. Receivers with HEMTs in common-source and cascode configuration were developed and compared with respect to their noise behavior and gain.

II. Transimpedance and Equivalent Input Noise Current

In this section, a short review will be given on how the intrinsic conductance of a photodiode can be used to calculate the equivalent input noise and quasi-optic transimpedance of a photoreceiver. The theory behind the intrinsic conductance is described in [8].

A. Transimpedance and Optoelectronic Conversion Gain

Fig. 1 shows an equivalent circuit of a photoreceiver consisting of a photodiode, a matching circuit and an amplifier.

As can be seen from Fig. 1, the photodiode is modeled by a current source followed by an equivalent circuit comprising a junction capacitance and resistance, and a series resistance. As the time required for photogenerated carriers to travel through the intrinsic region of the photodiode also affects the frequency response [10], two transfer functions are needed to describe the overall frequency response. The frequency dependent responsivity of a photodiode can be calculated to be

$$R = \frac{i_{p,\mathrm{ex}}}{P_{\mathrm{opt}}} = H_{TT} H_{\mathrm{EC}} \tag{1}$$

where P_{opt} denotes the incident optical power. The current $i_{p,\mathrm{ex}}$

is defined in Fig. 1. The transfer function

$$H_{TT} = \frac{i_p}{P_{\text{opt}}} \tag{2}$$

describes the finite carrier transit time in the photodiode absorption region. i_p can be regarded as the ideal short circuit photocurrent, if the photodiode parasitics are neglected.

If chain parameters $a_{ij,\,\text{PD}}$ are used to describe the parasitic elements of the photodiode, the transfer function of the photodiode equivalent circuit H_{EC} can be written as [8]

$$H_{\text{EC}} = \frac{i_{p,\,\text{ex}}}{i_p} = \frac{1}{a_{21,\,\text{PD}} Z_L + a_{22,\,\text{PD}}}. \tag{3}$$

If the transimpedance

$$Z_T = \left| \frac{v_L}{i_{p,\,\text{ex}}} \right| \tag{4}$$

of the amplifier including the matching network is known, the optoelectronic conversion gain C_{OE} can be calculated using the above introduced transfer functions

$$C_{\text{OE}} = \left| \frac{v_L}{P_{\text{opt}}} \right| = |H_{TT} H_{\text{EC}}| Z_T. \tag{5}$$

To facilitate the design of photoreceivers using standard circuit simulator tools, it is helpful to introduce a so-called quasi-optic transimpedance [11]

$$Z_{T,\,\text{qopt}} = \left| \frac{v_L}{i_p} \right| = |H_{\text{EC}}| Z_T. \tag{6}$$

This quasi-optic transimpedance is very useful as no optical power source needs to be modeled within the circuit simulator.

In [8], it was shown that the quasi-optic transimpedance and the optoelectronic conversion gain can easily be calculated by using the intrinsic conductance $G_{i,\,\text{PD}}$ of the photodiode, if the matching network is reciprocal and lossless as follows:

$$Z_{T,\,\text{qopt}} = \frac{1}{2} \sqrt{G_T \frac{Z_0}{G_{i,\,\text{PD}}}} \tag{7}$$

$$C_{\text{OE}} = \frac{1}{2} |H_{TT}| \sqrt{G_T \frac{Z_0}{G_{i,\,\text{PD}}}} \tag{8}$$

where G_T and Z_0 denote the transducer power gain of the amplifier [14] and the characteristic impedance, respectively. As the transducer power gain is dependent on the reflection coefficient at the input of the amplifier, see Fig. 1, Γ_m can be used for tuning the photoreceiver to the desired frequency response by using any of the well known techniques for network synthesis, see, e.g., [12], [13]. For instance it is possible to plot circuits of constant quasi-optic transimpedance or constant optoelectronic conversion gain in a Smith chart. The equations for circle center $C_{C_{\text{OE}}}$ and circle radius $r_{C_{\text{OE}}}$ are as follows:

$$C_{C_{\text{OE}}} = \frac{x S_{11}^*}{1 - |S_{11}|^2 (1 - x)} \tag{9}$$

$$r_{C_{\text{OE}}} = \frac{\sqrt{1 - x}\,(1 - |S_{11}|^2)}{1 - |S_{11}|^2 (1 - x)}. \tag{10}$$

The parameter x is the squared ratio of the chosen and the maximum value of conversion gain or quasi-optic transimpedance, respectively,

$$\begin{aligned} x &= Z_{T,\,\text{qopt},\,0}^2 \frac{4 G_{i,\,\text{PD}} \left(1 - |S_{11}|^2\right)}{Z_0 |S_{21}|^2} \\ &= \frac{C_{\text{OE},\,0}^2}{|H_{TT}|^2} \frac{4 G_{i,\,\text{PD}} \left(1 - |S_{11}|^2\right)}{Z_0 |S_{21}|^2}. \end{aligned} \tag{11}$$

The subscript 0 denotes the value for which the circle is to be drawn. Equations (9) and (10) are equal to the equations for constant-gain circles, which can be found in [14].

B. Equivalent Input Noise Current

As the matching circuitry is assumed to be reciprocal and lossless, no noise arises from the matching network. The only sources for noise that can be influenced by the designer is thermal noise from the photodiode parasitics and noise from the amplifier. All these noise sources can be transformed into a current noise source i_{eq} in parallel to the input current source as can be seen from Fig. 1. This allows us to compare this noise with other sources of noise such as the quantum or shot noise that arises during the statistical process of the generation of electron-hole pairs or noise from the optical source. The equivalent input noise current can be calculated as follows [8]:

$$\overline{|i_{\text{eq}}|^2} = 4 k T_0 df G_{i,\,\text{PD}} F \tag{12}$$

where k, T_0, and df is Boltzmann constant, the reference temperature, and the differential bandwidth, respectively. F denotes the noise figure of the amplifier, which is dependent on the reflection coefficient Γ_m [14]. For a given photodiode and amplifier, the equivalent input noise current is only dependent on the reflection coefficient Γ_m. Therefore, we can plot circles of constant equivalent input noise current on a Smith chart (Γ_m-plane). The equations for center $C_{i_{\text{eq}}}$ and radius $r_{i_{\text{eq}}}$ of such a circle are identical to the ones for circles of constant noise figure (see [14])

$$C_{i_{\text{eq}}} = \frac{\Gamma_{\text{opt}}}{1 + y} \tag{13}$$

$$r_{i_{\text{eq}}} = \frac{1}{1 + y} \sqrt{y^2 + y(1 - |\Gamma_{\text{opt}}|^2)} \tag{14}$$

where

$$y = \frac{\overline{|i_{\text{eq},\,0}|^2} - \overline{|i_{\text{eq,\,min}}|^2}}{16 k T_0 G_{i,\,\text{PD}} r_n} |1 + \Gamma_{\text{opt}}|^2 \tag{15}$$

is a parameter proportional to the difference between the squared equivalent input noise current $i_{\text{eq},\,0}$ for which the circle is to be drawn and the squared minimum achievable equivalent input noise current, given by

$$\overline{|i_{\text{eq,\,min}}|^2} = 4 k T_0 df G_{i,\,\text{PD}} F_{\text{min}}. \tag{16}$$

F_{min}, $r_n = R_n / Z_0$ and Γ_{opt} denote minimum noise figure, normalized noise resistance and optimum source reflection coefficient of the amplifier.

III. Extraction of the Intrinsic Conductance

As can be seen from (7) and (12), transimpedance is inversely proportional, and equivalent input noise current is proportional, to the square root of the photodiode intrinsic conductance. In [8] it was shown, that the intrinsic conductance can be calculated from the two-port parameters of the photodiode equivalent circuit. If chain parameters $a_{ij,\,\mathrm{PD}}$ are used, the intrinsic conductance can be calculated to be

$$G_{i,\,\mathrm{PD}} = \mathrm{Re}\{a_{21,\,\mathrm{PD}}^{*} a_{22,\,\mathrm{PD}}\}. \tag{17}$$

Basically, two methods exist to determine the intrinsic conductance of a given photodiode. Both methods rely to a certain extent on modeling a part of the photodiode behavior. Both methods are described and compared in the following sections.

A. Transfer Function Method

According to (3), the transfer function H_{EC} can be calculated from the chain parameters of the equivalent circuit. The photodiode output conductance can also be expressed in terms of chain parameters:

$$Y_{\mathrm{PD}} = \frac{1}{Z_0}\frac{1-\Gamma_{\mathrm{PD}}}{1+\Gamma_{\mathrm{PD}}} = \frac{a_{21,\,\mathrm{PD}}}{a_{22,\,\mathrm{PD}}} \tag{18}$$

where Γ_{PD} is the photodiode reflection coefficient (see Fig. 1). If both the transfer function H_{EC} and the photodiode output conductance are known, the two chain parameters $a_{21,\,\mathrm{PD}}$, $a_{22,\,\mathrm{PD}}$ and, using (17), also the photodiode intrinsic conductance can be calculated.

While the reflection coefficient can be easily measured using a network analyzer, this is more difficult for the transfer function H_{EC}. According to (1), H_{EC} can be calculated from the photodiode responsivity, if H_{TT} is known. There are two problems that have to be taken into account. First, the responsivity is depending on the load impedance, with which the responsivity was measured. One has to assure that the load impedance used for measurement is the same as the input impedance of the amplifier. The second problem is that it is difficult, especially at higher frequencies, to determine the phase of the responsivity very accurately. Substituting (3) and (18) into (17) yields an expression for $G_{i,\,\mathrm{PD}}$, that is only dependent on the magnitude of H_{EC} as follows:

$$G_{i,\,\mathrm{PD}} = \left|\frac{Y_{\mathrm{PD}}}{H_{\mathrm{EC}}(Z_L Y_{\mathrm{PD}}+1)}\right|^2 \mathrm{Re}\left\{\frac{1}{Y_{\mathrm{PD}}}\right\}. \tag{19}$$

Therefore, it is sufficient to measure the magnitude of the responsivity and the complex output conductance to model the transfer function H_{TT}.

B. Equivalent-Circuit Method

Another approach to determine the intrinsic conductance is to find an equivalent circuit that is a good representation of the transfer function H_{EC}. If an equivalent circuit is used like the one depicted in Fig. 1 consisting of a junction capacitance C_i, a parallel resistance R_i and a series resistance R_s, then the intrinsic conductance is given by

$$G_{i,\,\mathrm{PD}} = \frac{R_s+R_i}{R_i^2} + (\omega C_i)^2 R_s. \tag{20}$$

Parameter extraction can be done by measuring the complex reflection coefficient of the photodiode and fitting the model to the measured data. This second method is recommended if the photodiode can be accurately described by a few equivalent circuit elements as in the example given above. If it is difficult to find a valid equivalent circuit, the first method should be used.

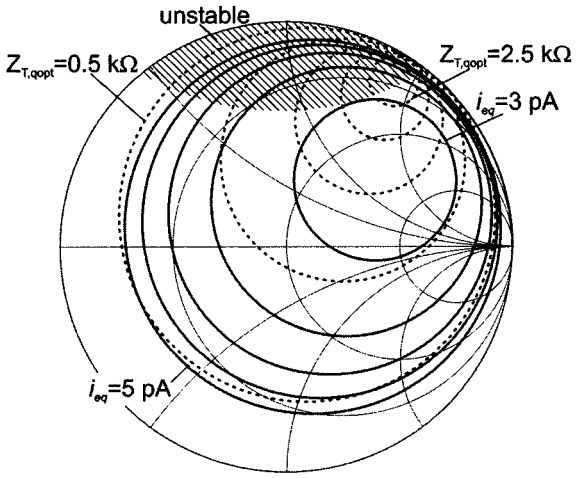

Fig. 2. Circles of constant quasi-optic transimpedance (broken line) and constant equivalent input noise current per square-root hertz at 10 GHz.

IV. Application: 10-GHz Narrow-Band Photoreceivers

In this section, it is presented how the techniques described above are used to design monolithic integrated narrow-band photoreceivers at 10 GHz. Due to the absence of bonding parasitics between photodiode and amplifier, monolithic integration can show the full potential of this matching technique. Details on technology and the fabrication of the photoreceivers described here can be found elsewhere [15], [16].

A. Circuit Design

To design a photoreceiver using the technique described here, the photodiode intrinsic conductance has to be determined. If a simple equivalent circuit as depicted in Fig. 1 is chosen, the following parameters can be extracted for a photodiode with a light-sensitive area of 10-μm diameter: $C_i = 112.2$ fF, $R_s = 8.3\ \Omega$, $R_i = 10$ kΩ. From (20), the photodiode intrinsic conductance $G_{i,\,\mathrm{PD}}$ is 0.51 mS at 10 GHz. Using (9)–(11) and (13)–(15), circles of constant quasi-optic transimpedance and constant equivalent input noise current can be drawn in a Smith chart. The result for the above described photodiode is depicted in Fig. 2. The transistor parameters are given in Table I. These parameters were extracted for a 0.15-μm gate-length HEMT in cascode configuration with a gatewidth of $2 \times 60\ \mu$m for each, the common-gate and the common-source part of the transistor.

In Fig. 2, the hatched area corresponds to regions of unstable transistor operation. Outside of this unstable area, an input reflection coefficient can be chosen that results in a

TABLE I
TRANSISTOR PARAMETERS FOR EQUIVALENT INPUT NOISE CURRENT AND TRANSIMPEDANCE CIRCLES CALCULATION

Parameter	Symbol	Value
Minimum noise figure	F_{min}	0.91 dB
Noise resistance	R_n	19.1 Ω
Optimum source reflection coefficient	Γ_{opt}	0.48 + j 0.36
Scattering parameters	S_{11}	0.51 - j 0.79
	S_{21}	-4.45 + j 5.29

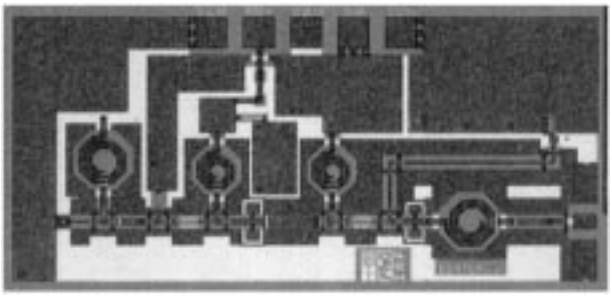

Fig. 3. Chip photograph of the two-stage photoreceiver with HEMTs in common-source configuration.

compromise between transimpedance and noise. As these values for quasi-optic transimpedance and equivalent input noise current are given for a single device, these values can not be obtained for a complete photoreceiver, as losses in the matching networks reduce the overall performance. Furthermore, out-of-band stability and a certain bandwidth have to be assured, increasing noise and reducing transimpedance.

Using the design technique described here, one- and two-stage photoreceivers were designed and produced. Circuit design was performed using commercially available microwave design software. To predict the transimpedance and noise behavior accurately, a large signal HEMT model [17] was used, which also allows simulation of the bias dependent noise parameters of the HEMT [18].

Fig. 3 shows a chip photograph of the two-stage photoreceiver with HEMTs in common-source configuration. In both stages, 0.15 μm gate-length HEMTs with a width of 2 $\times$ 60 μm were used. To minimize the circuit size, the input matching network between the photodiode and the first transistor as well as the interstage and output matching network consist of a combination of coplanar transmission lines, metal–insulator–metal (MIM) capacitors, and airbridge inductors. For gate biasing of the first transistor, a 2-kΩ resistor is used. This resistor also ensures out-of-band stability at the expense of a increased equivalent input noise current. The total chip size of this photoreceiver is 1 $\times$ 2 mm^2, including RC bias networks.

The topology of the two-stage photoreceiver with HEMTs in cascode configuration is similar to the photoreceiver with common-source transistors. But this design provides nearly twice as much gain as a common-source transistor with a even reduced chipsize (1 $\times$ 1.5 mm^2). Besides this, at 10 GHz, the gain of the common-source part of the cascode transistor is so high, that the common-gate part has nearly no influence on the overall noise figure of the total device.

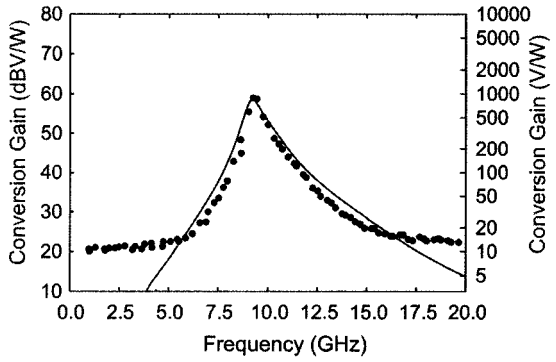

Fig. 4. Measured optoelectronic conversion gain of the two-stage photoreceiver with HEMTs in common-source configuration (circles) and simulation (line).

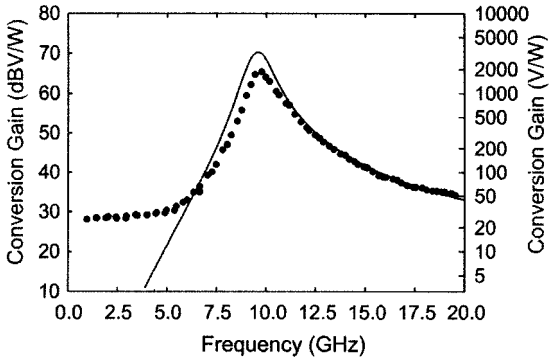

Fig. 5. Measured optoelectronic conversion gain of the two-stage photoreceiver with HEMTs in cascode configuration (circles) and simulation (line).

B. Measurement Results

The optoelectronic conversion gain as a function of frequency for both photoreceivers is depicted in Figs. 4 and 5. Filled circles represent measurement results, which are obtained using an optical heterodyne setup [19] based on two external cavity tunable diode lasers and a wide bandwidth RF power sensor. The optical input power is chosen such that the photoreceivers are in a linear operating regime. At 10 GHz, an optoelectronic conversion gain of 468 V/W (53.4 dBV/W) and 1600 V/W (64.1 dBV/W) is achieved for the common-source and the cascode photoreceiver, respectively. Due to the noise matching, the maximum conversion gain is shifted to a slightly lower frequency.

Figs. 4 and 5 also include simulated data. These data are calculated using (8) and the photodiode intrinsic conductance according to (20). The transfer function H_{TT} is assumed to be equal to the dc responsivity of 0.3 A/W. This assumption is permitted because the 3-dB cutoff frequency of H_{TT} is as high as 72 GHz for a 400-nm-thick InGaAs absorption layer. A good agreement between measurement and simulation can be seen. For low conversion gains, the noise floor of the measurement setup causes a measurement error such that the measured data give a higher conversion gain than the simulation. Fig. 5 shows an approximately 3 dB lower measured peak conversion gain than simulated. That is due to a difference in the output reflection coefficient of the cascode transistor model and measurement. Therefore, the interstage matching network is detuned resulting in a reduced peak conversion gain.

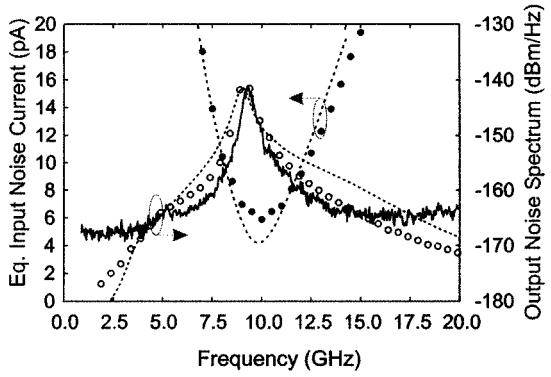

Fig. 6. Equivalent input noise current per square-root hertz and output noise spectrum of the two-stage photoreceiver with common-source transistors. Line: measured noise spectrum; circles: data extracted from noise parameter measurements; broken lines: simulation.

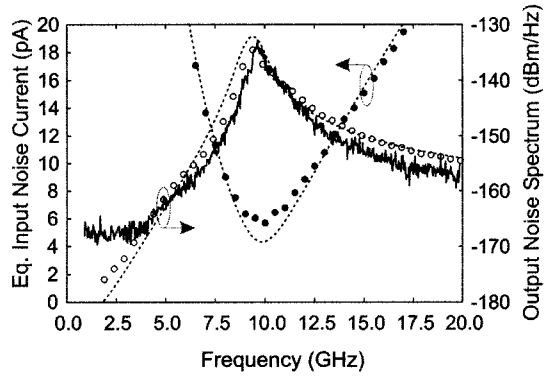

Fig. 7. Equivalent input noise current per square-root hertz and output noise spectrum of the two-stage photoreceiver with cascode transistors. Line: measured noise spectrum; circles: data extracted from noise parameter measurements; broken lines: simulation.

Noise performance of the photoreceivers is determined in two different ways. To verify the models, amplifiers with RF input pads instead of photodiodes were fabricated on the same wafer. By measuring all noise parameters of that amplifier and using (12) and (20), the equivalent input noise current for a complete photoreceiver is calculated. The result is depicted in Figs. 6 and 7 as filled circles and compared with simulations. At 10 GHz, an equivalent input noise current of 5.9 and 5.7 pA per square-root hertz was extracted for the photoreceivers with common-source and cascode transistors, respectively. The difference of 0.2 pA lies within the uncertainties of this measurement method. The very good agreement between measurement and simulation proves the validity of the models, especially those used for the transistors.

The second method to determine the noise behavior of the photoreceivers is to measure the output spectral noise power using low noise spectrum analyzer. These results are also depicted in Figs. 6 and 7. At 10 GHz, the output noise power density is -148 and -135 dBm/Hz for the photoreceiver using common-source and cascode transistors, respectively. Also included are the output noise power densities calculated by multiplying the measured equivalent input noise currents with quasi-optic transimpedances, calculated from measured scattering parameters. All measured results show excellent agreement with simulations, which are depicted in Figs. 6 and 7 as broken lines. All simulations were performed using a commercial circuit design tool (HP MDS). No model adjustment was done after circuit fabrication.

V. Conclusion

The design of 10-GHz narrow-band photoreceivers with a very low equivalent input noise current of 5.7 pA per square-root hertz and a high optoelectronic conversion gain of 64.1 dBV/W is demonstrated. The excellent agreement between simulation and measurement shown in Section IV-B proves not only the validity but also practicality of the photodiode intrinsic conductance as a versatile parameter for designing photoreceivers.

Acknowledgment

The authors would like to thank K. Köhler for MBE growth, W. Bronner for technology and sample preparation, and M. Schlechtweg and G. Weimann for their continuing support.

References

[1] W. D. Jemison, P. R. Herczfeld, W. Rosen, A. Vieira, A. Rosen, A. Paolella, and A. Joshi, "Hybrid fiberoptic millimeter-wave links," *IEEE Microwave Mag.*, vol. 1, pp. 44–51, 2000.

[2] H. J. Carlin, "A new approach to gain-bandwidth problems," *IEEE Trans. Circuits and Syst.*, vol. CAS-24, pp. 170–175, 1977.

[3] J. L. Gimlett, "Low-noise 8 GHz PIN/FET optical receiver," *Electron. Lett.*, vol. 23, pp. 281–283, 1987.

[4] K. Ogawa, "Noise caused by GaAs MESFETs in optical receivers," *Bell Syst. Tech. J.*, vol. 60, pp. 923–928, 1981.

[5] M. S. Park and R. A. Minasian, "Ultra-low-noise and wideband-tuned optical receiver synthesis and design," *J. Lightwave Technol.*, vol. 12, pp. 254–259, Feb. 1994.

[6] M. Schneider, "Reduction of spectral noise density in p-i-n-HEMT lightwave receivers," *J. Lightwave Technol.*, vol. 9, pp. 887–892, July 1991.

[7] K. E. Alameh and R. A. Minasian, "Tuned optical receivers for microwave subcarrier multiplexed lightwave systems," *IEEE Trans. Microwave Theory Tech.*, vol. 38, pp. 546–551, May 1990.

[8] A. Leven, R. Reuter, and Y. Baeyens, "Unified analytical expressions for transimpedance and equivalent input noise current of optical receivers," *IEEE Trans. Microwave Theory Tech.*, vol. 48, pp. 1701–1706, Oct. 2000.

[9] P. J. Matthews, "Practical photonic beamforming," in *Proc. Int. Microwave Photon. Topical Meeting*, 1999, pp. 271–274.

[10] J. E. Bowers and C. A. Burrus, "Ultrawide-band long-wavelength p-i-n photodetectors," *J. Lightwave Technol.*, vol. JT-5, pp. 1339–1350, 1987.

[11] S. van Waasen, "Wanderwellenverstärker für hochbitratige monolithisch integrierte Photoempfänger auf Basis von InAlAs/InGaAs/InP-Heterostruktur-Feldeffekttransistoren," Ph.D. dissertation, Gerhard-Mercator-Universität Duisburg, Duisburg, Germany, 1999.

[12] M. W. Medley, *Microwave and RF Circuits: Analysis, Synthesis and Design*. Norwood, MA: Artech House, 1992.

[13] B. J. Minnis, *Designing Microwave Circuits by Exact Synthesis*. Norwood, MA: Artech House, 1996.

[14] G. Gonzales, *Microwave Transistor Amplifiers*, 2nd ed. Englewood Cliffs, NJ: Prentice-Hall, 1997.

[15] W. Bronner, W. Benz, M. Dammann, P. Ganser, N. Grün, V. Hurm, T. Jakobus, K. Köhler, M. Ludwig, and E. Olander, "Monolithic integration of a GaInAs PIN photodiode and AlGaAs/GaAs/AlGaAs HEMT's on GaAs substrate," in *Proc. Int. Compound Semiconduct. Symp.*, 1997, pp. 383–386.

[16] V. Hurm, W. Benz, W. Bronner, A. Hülsmann, T. Jakobus, K. Köhler, A. Leven, M. Ludwig, B. Raynor, J. Rosenzweig, M. Schlechtweg, and A. Thiede, "40 Gbit/s 1.55 μm PIN-HEMT photoreceiver monolithically integrated on 3in GaAs substrate," *Electron. Lett.*, vol. 34, pp. 2060–2062, 1998.

[17] R. Osorio, M. Berroth, W. Marsetz, L. Verweyen, M. Demmler, H. Massler, M. Neumann, and M. Schlechtweg, "Analytical charge conservative large signal model for MODFET's validated up to mm-wave range," in *IEEE MTT-S Int. Microwave Symp. Dig.*, 1998, pp. 595–598.

[18] R. Reuter and A. Leven, "Analytical, scaleable large signal noise model for GaAs and InP MMIC applications," in *Proc. 29th European Microwave Conf.*, vol. 2, 1999, pp. 213–216.

[19] P. D. Hale, D. A. Humphreys, and A. D. Gifford, "Photodetector frequency response measurements at NIST, US, and NPL, UK: Preliminary results of a standards laboratory comparison," *Proc. SPIE*, vol. 2149, pp. 345–356, 1994.

Andreas Leven (S'97–M'01) received the Diploma degree and Dr.-Ing. degree in electrical engineering from the University of Karlsruhe, Karlsruhe, Germany, in 1997 and 2000, respectively.

In 1996, he joined the Optoelectronic Components Group, Fraunhofer-Institut für Angewandte Festkörperphysik, Freiburg, Germany, where he was involved with noise theory of optical receivers and the design of optical receivers for high-speed lightwave applications and microwave photonics. In 2000, he joined Lucent Technologies, Bell Laboratories, Murray Hill, NJ.

Volker Hurm was born in Schwäbisch Gmünd, Germany, in 1953. He received the Diploma degree in physics from the University of Tübingen, Tübingen, Germany, in 1979, and the Doctor of Science degree from the University of Freiburg, Freiburg, Germany, in 1983.

In 1979, he joined the Fraunhofer-Institut für Angewandte Festkörperphysik, Freiburg, Germany, where he was initially involved with the modeling and characterization of silicon devices. He was then engaged in the research and development of II–VI materials and the management of computer-aided-design (CAD) systems. He is currently involved in the development of monolithic and hybrid integrated photoreceivers for up to 40-Gbit/s digital transmission systems and up to 60-GHz microwave systems.

Ralf Reuter was born in Gelsenkirchen, Germany, on March 17, 1966. He studied electronics, with the main subject of microelectronics, and received the Diplom-Ingenieur and Dr.-Ing. degrees from the Gerhard-Mercator-University, Duisburg, Germany, in 1992 and 1998, respectively.

In 1997, he joined the Fraunhofer-Institut für Angewandte Festkörperphysik, Freiburg, Germany, where he heads the High Frequency Measurement and Characterization Group. His research interests and activities are in the field of simulation and modeling III–V semiconductor devices. He is also engaged in the investigation of new optimization algorithms based on the theory of evolution for modeling electronic devices. Since 2000, he has been with the Semiconductor Products Sector, Motorola, Berlin, Germany.

Josef Rosenzweig was born in Woschgaly, USSR, in 1946. He received the Diploma degree in physics (with honors) from the State University of Novosibirsk, Novosibirsk, USSR, in 1969, and the Doctor of Science and Habilitation degrees in physics from the University of Karlsruhe, Karlsruhe, Germany, in 1981 and 1987, respectively.

From 1969 to 1973, he was with the Institute of Semiconductor Physics, USSR Academy of Sciences, Novosibirsk, USSR, where he investigated microwave instabilities in III–V semiconductors at high electric and magnetic fields. From 1976 to 1981, he was a Research Assistant and, from 1981 to 1987, an Assistant Professor at the Institute of Applied Physics, University of Karlsruhe, where he studied bipolar photoconductivity, photo-Hall, and acoustoelectric effects in II–VI semiconductors. In 1987, he joined the Fraunhofer-Institut für Angewandte Festkörperphysik, Freiburg, Germany, where he is currently engaged in the development of high-speed optoelectronic devices and circuits based on III–V semiconductor compounds. He is also the Head of the Optoelectronics and Packaging Group.

Dr. Rosenzweig is a member of the German Physical Society.